Gravitational wakes in Saturn's rings

H. Salo

Department of Astronomy, University of Oulu, 90570 Oulu, Finland

THE outer parts of Saturn's rings display a variety of local non-uniformities in their particle distributions. Azimuthal brightness variations are seen in the A-ring[1,2], and may be attributable to the gravitational aggregation of particles into linear wakes that trail the rotation of the ring[3–5]; Voyager's stellar occultation experiments revealed large differences, on length scales as small as 150 m, in the surface density of particles[6]. Theoretical arguments[7,8] suggest that local instabilities may occur in both the A- and B-rings, the instability criterion depending on the velocity dispersion of ring particles and the orbital velocity and mass density in the ring. These arguments, however, are derived from the purely gravitational dynamics of an idealized, infinitesimally thin ring, made of identical particles. Here I use numerical simulations, including both gravitational interactions and dissipative impacts between particles, to study realistic models of Saturn's rings. For the C-ring there is no instability, but for the B- and A-rings gravitational wakes form. In the A-ring these wakes are so strong that particles trapped in them form metre-sized aggregate particles, which themselves lead to further instability. These different behaviours are consistent with the observational evidence.

The dynamical evolution of the main components of Saturn's rings is governed by the frequent impacts among the macroscopic icy particles; the local equilibrium state follows from the balance between dissipative energy loss in partially inelastic collisions and viscous gain of energy from the systematic velocity field. Laboratory measurements[9] indicate that collisions are very inelastic, with coefficient of restitution $\varepsilon < 0.5$, for impact velocities of only a few millimetres per second. Accordingly, purely collisional simulations predict little velocity dispersion at equilibrium, and therefore predict that the vertical thickness of the rings should only be only few times the dominant particle size. It is instructive to apply gravitational stability criteria to such idealized systems. According to Toomre[10], a differentially rotating, infinitely flat system is stable against all axisymmetric perturbations, as long as the radial velocity dispersion exceeds $\sigma_r > \sigma_{cr} = 3.36G\Sigma/\kappa$, where Σ denotes the surface mass density and κ the epicyclic frequency, equal to angular frequency Ω in a keplerian velocity field. For a system of identical particles each of density ρ and radius r, the surface density is related to normal optical thickness τ by $\Sigma = 4\rho r\tau/3$. Collisional simulations[11,12] indicate that $\sigma_r \approx 3r\Omega$ or smaller for any τ, and the stability criterion can thus be written $\tau_{cr} = 0.4(10^8/a\ \mathrm{m})^3 (0.9/\rho\ \mathrm{g\ cm^{-3}})$, giving the value of τ above which instability should occur at a distance a from the centre of Saturn. For the C-, B- and A-rings, $\tau_{cr} \approx 0.7$, 0.4 and 0.2, respectively, suggesting that although the C-ring, with mean $\tau \approx 0.15$, should be stable, both B- and A-rings ($\tau > 1.0$ and $\tau \approx 0.5$) might be susceptible to local instabilities.

This simple estimate for τ_{cr} should be considered with caution, as it ignores the increase of random velocities due to gravitational encounters[13–15]. In addition, recent collisional simulations with extended size distribution[16] indicate that σ_r can be as much as 5-fold for the smallest particles as compared with σ_r of the largest ones. This might stabilize at least their subpopulation, and possibly the whole system, by decreasing the effective surface density susceptible to perturbations. Any wakes formed would also scatter particles, and the net result might well be to alter the velocity dispersion in such a way that instabilities are eventually avoided[10].

Even if the axisymmetric Toomre stability criterion is fulfilled, systems with the ratio $Q_T = \sigma_r/\sigma_{cr}$ close to unity can still show a strong tendency to form transient density wakes. According to Julian and Toomre[17], these wakes appear in the form of trailing wavelets whose most prominent azimuthal wavelength is $\sim 2\lambda_{cr}$, where $\lambda_{cr} = 4\pi^2 G\Sigma/\kappa^2$ denotes the shortest axisymmetric wavelength stabilized by differential rotation alone. For Saturn's rings, $\lambda_{cr} \approx 70(a/10^8)^3(\Sigma/1{,}000)$, where a is in metres and Σ in kg m^{-2}, or about 6, 65 and 85 m for typical C-, B- and A-ring parameters. The expected pitch angle (angle between wavecrest and tangential direction) is ~10–15° for a keplerian velocity field, if the thickness of the system is negligible compared with λ_{cr}. At least for stellar systems, unless there is some external driving (for example in the form of an orbiting mass concentration), these wakes are rapidly damped[17]. Therefore, the formation of particle aggregates seems to be necessary to maintain persistent wakes. Formally, the classical Roche distance for ice particles $R_{Roche} = 136{,}500$ km, but Weidenshilling *et al.*[18] estimate that particle aggregates could form well inside R_{Roche}: in principle, a small particle can stick gravitationally to the surface of a slowly rotating large ice particle for $a >$ 70,000 km, or everywhere in the rings. As this estimate does not take into account the disrupting effects of collisions, however, the survival of particle aggregates is uncertain. On the other hand, external driving may not be necessary in the presence of dissipation: impacts cool the system continuously and thereby aid the amplification of new wakes (compare with stellar

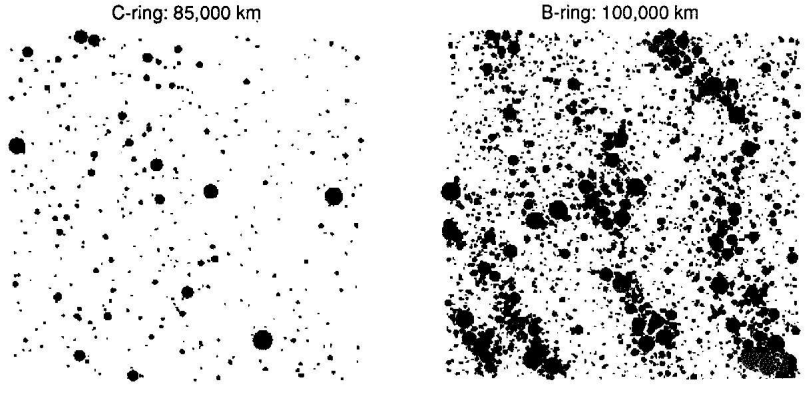

FIG. 1 Simulation for Saturn's C- and B-rings, for distances of $a = 85{,}000$ and 100,000 km from the centre of Saturn. I use the local simulation method[16], analogous to the stellar dynamical simulations of Toomre[20] and the planetary ring simulations of Wisdom and Tremaine[11]: all the calculations are restricted to a small co-moving cell inside the rings, with periodic boundary conditions taking into account the systematic shearing motion. Particle distributions after 10 orbital revolutions are displayed. The size distribution is approximated by a power-law with slope 3, extending over 50 cm $< r <$ 5 m, and each side of the (square) calculation cell is 170 m. Direction of the planet is to the left and mean orbital motion is upward. The gravitational force on each particle is calculated from all the other particles within 85 m. No softening is used, as the finite size of particles makes it unnecessary. Internal density of particles is taken to be $\rho = 0.9$ g cm^{-3}, and the surface densities are 120 and 960 kg m^{-2}, obtained by varying the total number of particles (400 and 3,200). For the coefficient of restitution, I assume a velocity-dependent elasticity model[9]: $\varepsilon(v_p) = (v_p/v_B)^{-0.234}$, $0.25 < \varepsilon < 1$, where v_p denotes the perpendicular component of impact velocity and $v_B = 0.01$ cm s^{-1}. Initially, random velocities correspond to equilibrium values in the non-gravitating case. The independence of the results from the cell size was checked by additional runs. The B-ring experiment required about 25 CPU hours on a IBM ES/9121-260 VF mainframe. Particle plots were produced by IDL software.

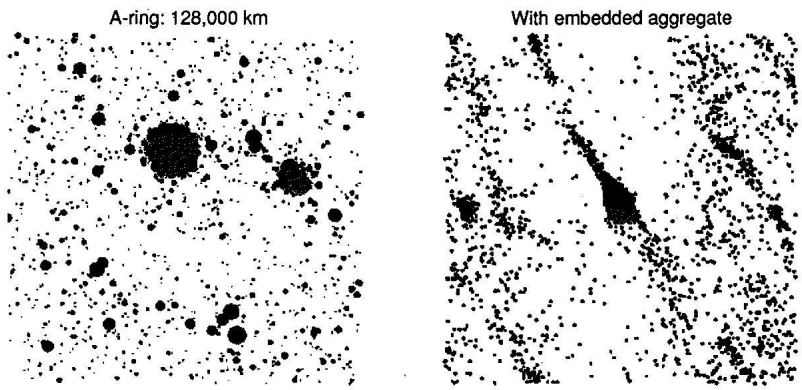

FIG. 2 Simulation model for Saturn's A-ring. The simulation on the left corresponds to Fig. 1, except that $a = 128{,}000$ km and $\Sigma = 480\ \mathrm{kg\ m^{-2}}$, obtained for 1,600 particles. The system is displayed after 10 orbital revolutions, when initial wakes have disappeared and ~30% of the mass has merged into single aggregate. On the right, the formed particle aggregate has been replaced by a single underdense particle with $r = 15$ m and $\rho = 0.3\ \mathrm{g\ cm^{-3}}$, embedded among 1,600 small particles with solid ice density and radius $r = 2$ m (total $\Sigma \approx 450\ \mathrm{kg\ m^{-2}}$). This reduces the computational burden considerably, as most of the CPU time in the previous experiment was spent in calculating the internal collisions among the particles constituting the aggregate. Width of the simulation cell is doubled (340 m) and the figure shows a snapshot of the system after 5 orbital revolutions.

dynamical simulations including cooling[19], where persistent spirals are maintained).

Because so many factors affect the dynamical state of rings, direct particle simulations offer the most reliable method for assessing the gravitational stability and possible presence of gravitational wakes. Figures 1 and 2 show gravitational simulations for three Saturnocentric distances corresponding to the C-, B- and A-rings. The elastic properties of particles follow laboratory measurements[9], and the size distribution is represented by a power law with slope 3, in accordance with Voyager measurements[21]. Although the distribution is truncated at the lower end, both the maximum particle size, which governs the velocity dispersion through gravitational encounters, and the local surface density, governing collective phenomena, should be fairly representative of those in the actual ring system (see ref. 22).

Figure 1 shows no trace of collective phenomena for the C-ring, because of its low surface density and because it is close to the planet. For the B-ring model, clear wakes are present. Inspection of the simulation system at various times shows that although individual wakes are transient phenomena and lose their identity in a few orbital periods, the overall density variations stay at roughly constant. The scale of these wakes seems to be consistent wih the Julian–Toomre estimate, although the pitch angle is about twice that expected for a strictly two-dimensional case, or ~30° instead of 15°. The velocity dispersion is roughly twice that seen in a similar run without self-gravity: for the largest particles the observed σ_r corresponds to $Q_T \approx 2$, and for the smallest, $Q_T \approx 3.5$. When gravity is included, the velocity dispersion shows fluctuations of ~30%, following the formation and disappearance of individual strong wakes.

For A-ring parameters, the behaviour is different. As for the B-ring, the initially cool system forms strong wakes within the first orbital revolution, but these wakes tend to collapse into elongated, almost radial particle groups, which may merge into a single aggregate (Fig. 2; aggregate size ~15 m). This behaviour confirms the proposed[18] rapid formation of aggregates, although it occurs only at the outer portions of the rings. In the case displayed, the aggregate is full of voids, and its final effective density is 30% of that of its constituent particles. Because of the lowered density, additional particles can no longer accumulate at its surface. In several additional runs, including particle spins and friction, and in models including more-elastic impacts, aggregates similar to that of Fig. 2 start forming at $a = 125{,}000$–$130{,}000$ km. Because the number of simulation particles is limited, it is difficult to estimate the actual maximum size possible if new particles were continuously available, and if the mutual collisions between aggregates were also included. Including centimetre-sized particles might also aid further growth as they could increase the mean density of the aggregates by filling the empty spaces between larger particles.

Figure 2 (right) displays another run for the A-ring, where the aggregate of the previous experiment has been treated as a single underdense particle. The size of the calculation cell has been doubled, and the wakes excited by the aggregate become visible. Also evident is the zone partially cleared by the massive particle. Compared with the previous B-ring model or the initial A-ring model, the pitch angle of wakes is reduced, especially at the inner edge of the gap.

These dynamical models are consistent with several observations. For example, the distinctly non-Poisson character of the photon noise in the Voyager stellar occultation measurement (PPS) indicates[6] that for the A-ring, the surface area locally covered by particles deviates significantly between successive measurement points. For the C-ring, uniform density is implied. The extra noise was explained by large maximum particle size, the variance arising from the presence or lack of large particle in each sampling area. According to our experiments, particles with size exceeding 10 m could be identified with the particle aggregates, without any need to revise the cut-off radius of the actual underlying particle distribution. The same explanation was also mentioned in ref. 6.

Dones and Porco[5] (see also Esposito[23]) have shown by light-scattering simulations that Julian–Toomre type wakes can in principle reproduce the observed azimuthal variations in A-ring brightness. Our model of wakes exited by an embedded aggregate (Fig. 2) should therefore be at least qualitatively consistent with the observations. Detailed photometric calculations would be needed to ascertain whether the present model correctly explains the brightness maximum at 165° from the superior conjunction. An unexpected new finding is the predicted wake structure in the B-ring, as no asymmetry has been measured. This could be due to the large optical depth: for example, Franklin and Colombo[24] note that even 10% variations in the surface density would not be detectable for this ring. Another possibility[23] is that the wakes are on a smaller scale than for the A-ring. Possible observational support for B-ring wakes is provided by the PPS measurement: according to Showalter and Nicholson[6], in these regions of B-ring that are not totally opaque, the implied variance is larger than elsewhere in the rings, suggesting structures on a scale of 20 m which would be roughly consistent with the simulated wakes. Dynamical arguments alone strongly suggest that B-ring wakes exist, unless the adopted standard models for $N(r)$, ε, Σ or ρ need serious revision. □

Received 8 June; accepted 17 August 1992.

1. Camichel, H. *Ann. Astrophys.* **21**, 231–242 (1958).
2. Thompson, W. K., Lumme, K., Irwine, W., Baum, W. & Esposito, L. *Icarus* **46**, 187–200 (1981).
3. Colombo, G., Goldreich, P. & Harris, A. W. *Nature* **264**, 344–345 (1978).
4. Franklin, F. A. *et al. Icarus* **69**, 280–296 (1987).
5. Dones, L. & Porco, C. *Bull. Am. astr. Soc.* **21** No. 3, 929 (1989).

6. Showalter, M. R. & Nicholson, P. D. *Icarus* **87,** 285–306 (1990).
7. Goldreich, P. & Tremaine, S. *A. Rev. Astr. Astrophys.* **20,** 249–283 (1982).
8. Salo, H. *Earth Moon Planets* **30,** 113–128 (1984).
9. Bridges, F. G., Hatzes, A. P. & Lin, D. N. C. *Nature* **309,** 333–335 (1984).
10. Toomre, A. *Astrophys. J.* **139,** 1217–1238 (1964).
11. Wisdom, J. & Tremaine, S. *Astr. J.* **95,** 925–940 (1988).
12. Salo, H. *Icarus* **90,** 254–270 (1991).
13. Cuzzi, J. N., Burns, J. A., Durisen, R. H. & Hamill, P. *Nature* **281,** 202–240 (1979).
14. Salo, H. *Earth, Moon Planets* **33,** 189–200 (1985).
15. Salo, H. *Earth, Moon Planets* **38,** 149–181 (1987).
16. Salo, H. *Icarus,* **96,** 85–106 (1992).
17. Julian, W. H. & Toomre, A. *Astrophys. J.* **146,** 810–830 (1966).
18. Weidenschilling, S. J., Chapman, C. R., Davis, D. R. & Greenberg, R. in *Planetary Rings* (eds Greenberg, R. & Brahic, A.) 367–415 (Univ. of Arizona Press, Tucson, 1984).
19. Sellwood, J. A. & Carlberg, R. G. *Astrophys. J.* **282,** 61–74 (1984).
20. Toomre, A. in *Dynamics and Interactions of Galaxies* (ed. Wielen, R.) 292–303 (Springer, Berlin, 1990).
21. Zebker, H. A., Marouf, E. A. & Tyler, G. L. *Icarus* **64,** 531–548 (1985).
22. Cuzzi, J. N. *et al.* in *Planetary Rings* (eds Greenberg, R. & Brahic, A.) 73–199 (Univ. of Arizona Press, Tucson, 1984).
23. Esposito, L. W. *Bull. Am. astr. Soc.,* **10** No. 3, 584–585 (1978).
24. Franklin, F. A. & Colombo, G. *Icarus* **33,** 279–287 (1978).